Eurasian Chem.-Technol. J. 27 (2025) 235–250
The journal of the Institute of Combustion Problems https://ect-journal.kz

https://doi.org/10.18321/ectj1671

ANN applied in the Separation of Isopropanol/Water by Azeotropic Distillation by Pressure Oscillation

Daniel Chuquín-Vasco[1]*, Adriana Castillo-Cevallos[2], Erika Cazorla-García[3], María Augusta Guadalupe[3], Geoconda Velasco-Castelo[3] and Fernando Mejía-Peñafiel[3]

[1]Universitat Politècnica de València, Valencia, España
[2]SOLMA, Advanced Mechanical Solutions, Mechanical Engineering, and Construction Services, Quito, Ecuador
[3]Escuela Superior Politécnica de Chimborazo (ESPOCH), Riobamba, Ecuador

Article info

Received:
4 June 2025

Received in revised form:
15 July 2025

Accepted:
28 August 2025

Keywords:
Artificial neural network (ANN)
DWSIM
Diisopropyl ether
Isopropanol
Simulation

Abstract

In this study, an artificial neural network (ANN) was developed to predict the concentrations of isopropanol (IPA) and diisopropyl ether (DIPE) in a pressure-swing azeotropic distillation system for the separation of isopropanol/water mixtures. To build the ANN, a simulation was validated using the open-source software DWSIM, and a sensitivity analysis was performed to determine the output variables (targets) to be predicted: IPA and DIPE molar fractions. Additionally, different experiments were carried out to obtain a set of 400 data pairs for the training and validation of the ANN. The design of the ANN was implemented in MATLAB, using the Bayesian regularization algorithm with 50 neurons in the hidden layer. The mean squared error obtained in the testing phase was 0.00186, and the regression coefficient was 0.964. To validate the ANN, an analysis of variance (ANOVA) was performed with a set of 25 data points, considering the input variables used in the ANN design. After the analysis of variance, it was concluded that the results predicted by the ANN did not present significant differences from the experimental values, with a reliability of 95%. Therefore, the developed ANN can be reliably used to predict the concentrations of IPA and DIPE in an isopropanol/water mixture separation process.

1. Introduction

The separation of azeotropic mixtures represents a significant challenge across various industrial sectors, especially in chemistry and pharmaceuticals. Azeotropes are combinations with a constant boiling point, making separation through conventional distillation complicated and resulting in products of low purity. A problematic example is the isopropanol-water azeotrope, which is found in numerous industrial applications.

Recently, efforts have been made to overcome the limitations of traditional distillation methods through the development of innovative and efficient techniques and technologies. One promising strategy is pressure swing distillation, which leverages variations in the liquid-vapor equilibrium under different pressures to separate azeotropic mixtures. By modifying pressure conditions during distillation, it's possible to overcome the azeotropic nature and improve separation efficiency [1].

To achieve optimal performance in pressure swing distillation and effectively separate isopropanol-water azeotropes, it's essential to incorporate advanced predictive tools. In this context, Artificial Neural Networks (ANNs) emerge as a prominent solution. ANNs are a branch of artificial intelligence specialized in modeling and predicting complex temporal data, making them particularly suitable for capturing the dynamic behavior of distillation systems.

*Corresponding author.
E-mail address: dachuvas@posgrado.upv.es

1.1. Isopropanol

Isopropanol (IPA), also known as 2-propanol or isopropyl alcohol, with the chemical formula C_3H_8O, is a versatile and economical solvent used in the chemical and cosmetic industries. Its physical characteristics, compatible with those of alcohol, water, and hydrocarbons, make it an invaluable resource. IPA serves as a primary ingredient in the production of acetone and various other compounds. It finds extensive use as an antiseptic and disinfectant for domestic, hospital, and industrial purposes [2].

1.2. Diisopropyl ether

Diisopropyl ether (DIPE) is an important component in the chemical industry, and its unique phase equilibrium properties allow the use of advanced distillation techniques like azeotropic distillation (HAD) and pressure-swing distillation (PSD) to achieve efficient separation, making it a favorable component in the distillation process [3]. In addition, due to its nonpolluting nature, DIPE represents a suitable candidate as a gasoline additive, supporting cleaner production processes [4].

1.3. Azeotrope

The term "azeotrope," derived from the Greek words "a" (without), "zeo" (to boil), and "tropos" (change), meaning "boiling without change," denotes a mixture of two or more components where the components remain at a constant temperature and pressure. An azeotrope is distinguished from a pure component by the fact that, upon variation of pressure, the boiling temperature and composition of the mixture change [5]

1.4. Distillation

Distillation is the primary method for purifying liquids, used to separate a liquid from unwanted non-volatile substances through vaporization. This separation process leverages variations in the vapor pressures of the mixture's components at a specified temperature. When liquid and gas phases interact during distillation, it's termed rectification, whereas in the absence of interaction between phases, it's called simple distillation. In the rectification zone, where phases interact, the gas phase increases its content of the most volatile component, while the liquid phase does so with the heavier component [6].

However, a major drawback of conventional distillation is its high energy consumption required for separating mixtures. Moreover, the significant emissions of CO_2 contribute to global warming. Therefore, enhanced distillation processes must be developed to address these issues, achieving energy-saving performance and environmental protection [7].

1.5. Azeotropic distillation

Separation based on distillation can become highly complex when attempting to separate highly non-ideal mixtures. While various unit operations have been successfully developed, there's always room for enhancing distillation techniques [8]

Process intensification represents a major prevailing trend in chemical process engineering for separating an azeotropic mixture. Azeotropic distillation is a technique employed to fractionate a compound exhibiting azeotropic behavior [9].

In separation processes, the topic of azeotropic mixtures generates considerable interest in the chemical industry, particularly in sectors where solvents are utilized. This is because a large number of solvents are involved in non-ideal systems that often result in the formation of azeotropes [10].

Azeotropic mixtures can be effectively separated through azeotropic or extractive distillation, accomplished by adding a substance known as a "carrier" to the distillation system. This addition facilitates the breakdown of azeotropes, making it an excellent choice for the separation and purification of the involved components [11].

1.6. Pressure swing azeotropic distillation

Pressure swing azeotropic distillation is widely utilized as an effective process for separating pressure-sensitive azeotropes in chemical industrial processes. This distillation method proves to be more cost-effective compared to traditional techniques such as extractive distillation, as it eliminates the need for an additional solvent to achieve breakdown. Pressure swing azeotropic distillation involves the separation of mixtures using two columns operating at varying pressures. To achieve this, a high-purity product is required at one end of the columns, while the other end utilizes a recycling stream with a composition close to the two azeotropes [12].

Pressure Swing Distillation (PSD) of azeotropic mixtures operates on the principle that a change in pressure can alter the relative volatility of a liquid mixture. As the operating pressure is increased, the

azeotropic point is shifted to lower the composition value of the lighter components, enabling separation without the need for separating agents when volatility increases and a significant positive change in the azeotropic point occurs [12].

1.7. Simulation for Isopropanol Separation

According to Buitrago et al. [13] chemical process simulation is a computer program employed to model steady-state behavior by determining pressures, temperatures, concentrations, and flow rates. In today's industry, one of the key tools is software that enables the creation of models and the execution of simulations of chemical and physical processes. The purpose of simulation software is to meet design requirements, decrease the required time, and reduce production costs.

The heuristic methodology proposed by Niu & Rangaiah [14] stands as an excellent option for optimizing operational conditions, comprising four steps: baseline case analysis, generation of an enhanced simulation without capital investment, generation of integrated solutions, and comparison of revamp solutions. This novel technology finds application in isopropanol (IPA) production, as it involves both primary and secondary reactions governed by chemical equilibrium. Consequently, its separation process encompasses intricate reactions. The simulation of IPA is conducted using Aspen Plus, where a stream of fresh propylene enters at (-47.6°C and 101.325 kPa), and recycled propylene is mixed in a molar ratio of 4.65:1. These streams are pressurized and preheated before entering the trickle bed reactor. Meanwhile, another reactive water stream is pressurized to 7500 kPa to feed the reactor. Two variables were considered in this process: excess propylene, where the number of columns has been reduced from seven to three with the new method, and excess water, with five columns.

To enhance the overall efficiency of the process, Chua et al. [2] propose using reactive distillation for IPA production in two different ways: employing an excess of propylene to generate pure IPA without the need for waters below the azeotropic mixture, albeit this alternative is highly challenging and costly; and with excess water, which requires further separation of IPA and water involving an azeotrope to avoid propylene-propane separation, thus achieving nearly complete propylene conversion.

According to Xu et al. [15], process design for isopropanol manufacturing employed MESH equations (material balance, vapor-liquid equilibrium, summation of molar fractions, and energy balance). Propylene hydration and ether, to obtain IPA, are fed to a catalyst bed. The UNIFAC method has been successfully used to predict activity coefficients in the liquid phase and equilibrium constant expressions for non-ideal systems. The Redlich-Kwong equation of state was utilized to predict the non-ideal vapor phase behavior of the system. Aspen Plus software has been successfully employed in catalytic distillation, where easier convergent results were obtained for the propylene hydration process, utilizing the integrated RadFrac distillation unit to gather all process data informatively.

In order to produce IPA, Arifin & Chien [16] propose a distillation/absorption process for separating binary liquid mixtures with homogeneous azeotropes. They utilized the commercial steady-state simulator Aspen Plus to perform mass and energy balances (mass and energy transfer equations, and the equilibrium isotherm). They integrated the continuous distillation process with cyclic absorption processes, using average quantities corresponding to the Aspen ADSIM cycle as feed flow rates to the Aspen Plus distillation columns.

In order to separate IPA and diisopropyl ether (DIPE), Guang et al. [17] propose employing extractive distillation, which offers enhanced control capabilities by incorporating a solvent to separate this mixture. However, introducing a solvent could potentially cause significant environmental damage.

1.8. ANN applied to chemical processes

Neural networks (ANNs) are a form of artificial intelligence inspired by the human brain, involving deep learning through interconnected neurons. This adaptable system enables computers to recognize errors and improve decision-making with minimal human intervention [18–24]. Over recent decades, ANNs have become a powerful tool in scientific and engineering, excelling at predicting complex, nonlinear phenomena. By processing nonlinear relationships and mapping complex input-output rules, ANNs offer practical solutions to intricate problems, emulating brain functions [25–29].

The application of ANNs in the industrial realm of chemical processes offers several advantages, notably high efficiency and rapid results attainment. Artificial neural networks provide a variety of novel techniques to address issues in sensor data analysis, fault detection, and process control, being utilized in chemical engineering [30].

According to Panerati et al. [31], ANNs are considered a highly powerful tool assisted by artificial intelligence. Chemical engineers have utilized this tool for countless applications over the years. Artificial neural networks are computational tools that provide a minimalist mathematical model of functional neurons alongside raw data through a learning algorithm. They can be employed for tasks such as modeling, classification, and prediction. Chemical engineers have applied ANN in a wide range of fields including energy, industrial chemical production, food, pharmaceuticals, biotechnology, and water. For instance, Cristea et al.[32] developed ANN models to predict the sorption capacity of a carbonized rice husk–shungite mixture in oil-contaminated soils, achieving high predictive accuracy (R^2 up to 0.998) and demonstrating strong interpolation capability.

Two main uses of ANNs stand out: determining the characteristics of an industrial process (yield, efficiency, etc.), the final properties of products, and analyzing quantitative structure-activity relationships. Within the chemical industry to produce all derivatives, the most employed type of ANN in the industry is the Multilayer Perceptron (MLP), with a smaller proportion utilizing Support Vector Machines, Generalized Regression Neural Networks (GRNN), Functional Neural Networks, and Radial Basis Function Neural Networks (RBFNN), based on supervised training algorithms. Himmelblau [33], designed a knowledge base with simulations to enhance reservoir characteristics and design scenarios by implementing artificial neural networks.

In recent years, Advanced Process Control (APC), such as Model Predictive Control (MPC), has been introduced in the chemical process industry to enhance operational efficiency. Shin et al. [34] utilized a linear model to predict computer workload for simulation and improvement over a long period, but high accuracy was not achieved in the supervision system of a distillation column. Therefore, an artificial neural network (ANN) model was adopted instead of the linear model to increase optimization speed and model accuracy. In the present study, a depropanizer was simulated using Aspen HYSYS software, considering all feasible operating scenarios to generate massive dynamic simulation data. An optimization algorithm model was incorporated into the MPC system to assess its performance, changes were made to the setpoint, and disturbances were applied to the model, comparing the efficiency of MPC with conventional control, such as PID feedback.

To enhance crude distillation systems with integrated heat, Ochoa-Estopier et al. [35] considered a novel approach in their study. They employed an artificial neural network model to depict a distillation tower, where the tower configurations and heat exchangers are tailored to an optimization framework, systematically defining operational conditions that contribute to the economic improvement of production.

This work stems from the scarcity of previous research utilizing Artificial Neural Networks (ANNs) for predictive purposes in pressure swing distillation of the isopropanol/water mixture. The lack of studies underscores the originality and relevance of applying ANN methodologies to this industrial process. Leveraging the predictive capabilities of neural networks in extractive distillation can enhance efficiency, optimize operational parameters, and provide valuable insights into the separation of isopropanol/water. Moreover, its significance extends beyond prediction, as it lays the groundwork for future research addressing hybrid energy optimization methodologies, combining genetic algorithms and neural networks.

2. Methodology

2.1. Process description

Figure 1 depicts the process for isopropanol separation based on the proposal by [17]. The main equipment includes distillation columns, decanters, pumps, and reboilers to achieve the required process temperatures and pressures.

Fresh feed (F) of water/IPA/DIPE enters the top tray of column CSCOL-1, operating at 1 atm pressure, where water is removed as a bottom product. When the overhead vapor (V3) from the high-pressure column (CSCOL-3) mixes with the overhead vapor (V1) from the low-pressure column (CSCOL-1), a heterogeneous liquid stream is created, feeding the decanter (Dec-1) after cooling the aqueous liquid (Lac) returns to the top tray of the low-pressure column (CSCOL-1), and the organic liquid feeds the intermediate tray of the low-pressure column (CSCOL-2). Isopropanol product is obtained at the bottom of the column (CSCOL-2). The distillate (D2) feeds the top of the column (CSCOL-3), while high-purity DIPE is obtained in column (CSCOL-3) as a bottom product (B3), and this is recycled V3.

Table 1. Feed stream conditions

Parameter	Value	Unit
Pressure	1	atm
Temperature	298.2	K
Feed (molar flow)	100	kmol/h
IPA - Mole fraction	0.70	-
DIPE - Mole fraction	0.30	-
Initial water composition	90	%

Source: [17]

Table 2. CSCOL -1 operating parameters

Parameter	Value	Unit
Pressure	1	atm
Theoretical trays number	5	-
Feed tray location	1	-
Feed flow	100	kmol/h
IPA - Mole fraction (distillate)	0.36	-
IPA - Mole fraction (bottom)	0.00045	-
DIPE - Mole fraction (distillate)	0.147	-
DIPE - Mole fraction (bottom)	0.00005	-
Water - Mole fraction (distillate)	0.49	-
Water - Mole fraction (bottom)	0.99	-
Distillate molar flow	21.2	kmol/h
Lower molar flow	9	kmol/h
Thermal load on the condenser	612.7	K
Thermal load on the reboiler	414.2	K

Source: [17]

Table 3. CSCOL -2 operating parameters

Parameter	Value	Unit
Pressure	1	atm
Theorical trays number	21	-
Feed tray location	3	-
Feed flow	36.8	kmol/h
IPA - Mole fraction (distillate)	0.1225	-
IPA - Mole fraction (bottom)	0.999	-
DIPE - Mole fraction (distillate)	0.6583	-
DIPE - Mole fraction (bottom)	0.0002	-
Water - Mole fraction (distillate)	0.2191	-
Water - Mole fraction (bottom)	0.0009	-
Thermal load on the condenser	550.3	K
Thermal load on the reboiler	609.2	K
Reflux ratio	0.991	-

Source: [17]

Table 4. CSCOL -3 operating parameters

Parameter	Value	Unit
Pressure	5	atm
Theoretical trays number	9	-
Feed tray location	1	-
Feed flow	29.793	kmol/h
IPA - Mole fraction (distillate)	0.136	-
IPA - Mole fraction (bottom)	0.0005	-
DIPE - Mole fraction (distillate)	0.620	-
DIPE - Mole fraction (bottom)	0.999	-
Water - Mole fraction (distillate)	0.244	-
Water - Mole fraction (bottom)	0.0008	-
Distillate molar flow	26.8	kmol/h
Bottom molar flow	2.993	kmol/h
Thermal load on the reboiler	318.0	K

Source: [17]

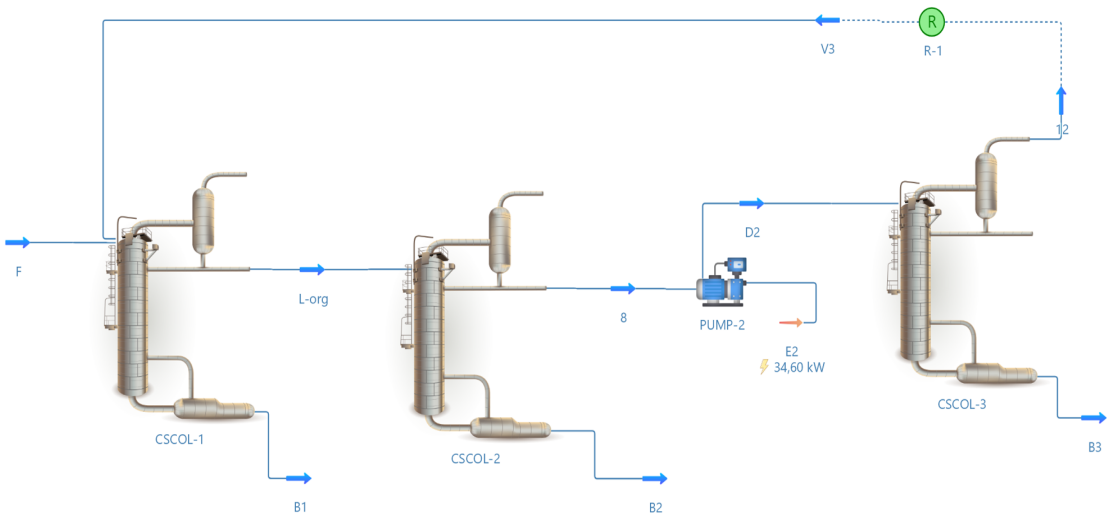

Fig. 1. Simulation of IPA separation by pressure swing in DWSIM Source: Modified from [17].

2.2. Methodology

The first part of the study involves simulating the process depicted in Fig. 1, based on the input flow conditions and equipment parameters specified in Tables 1-4. Subsequently, a sensitivity analysis is conducted to determine the input and output variables to be used for constructing the ANN. Finally, the ANN is trained and validated through statistical analysis to assess its predictive capability. Figure 2 illustrates the methodological framework employed for ANN design.

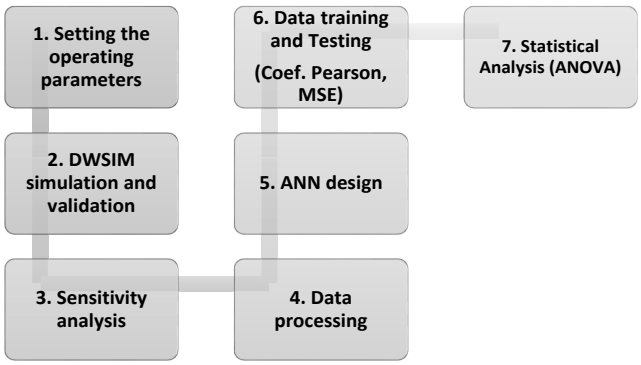

Fig. 2. Methodological scheme of the designed ANN.

2.3. DWSIM simulation

The proposal is developed using the Open-Source DWSIM software, which has a graphical user interface that allows comparison of different types of chemical processes. DWSIM was employed to reproduce the behavior of the improved isopropanol separation process. By systematically varying the operating parameters, a database of 400 data pairs was generated, which was subsequently used to train, test, and validate the ANN.

All flow streams are operated using the modified UNIQUAC property package. These models enable the accurate depiction of the non-ideality of the liquid system through the calculation of activity coefficients of the liquid and the modeling of the vapor phase [36–40].

2.4. Sensitivity analysis

A sensitivity analysis is carried out to determine the choice of input and output variables in an ANN, aiming to evaluate the relative importance of these variables. This analysis helps identify the most relevant features while discarding irrelevant ones, refining the architecture, and identifying potential issues. To perform this assessment, potential manipulated variables were identified, and ranges of variation were established based on the physical-chemical principles of the actual process.

2.5. ANN design and training

Training an ANN involves adjusting the connection weights between neurons to enable accurate predictions regarding the target output data. Validation is then utilized to measure the prediction errors of the ANN, thus assessing its effectiveness. Conversely, during the testing phase, the ANN's predictions are evaluated using data pairs not employed during training.

In the literature, ANNs uses a minimum of 50 data points for predictive regression algorithms [41–43]. In this work, the dataset generated in Section 2.3 (400 data pairs, see Appendix A) was employed for ANN design, ensuring an adequate basis for training, testing, and validation. The ANN was implemented in MATLAB as a feed-forward multilayer perceptron (MLP), which is widely applied due to its flexibility in nonlinear regression tasks [44]. Conforming to the guidance provided by Chen et al. [45], 70% of the entire dataset (comprising 280 data sets) was utilized for training and learning purposes. Meanwhile, the remaining 30% (120 data sets) was designated for testing to evaluate the ANN's learning capability.

2.6. ANN validation

To validate the artificial neural network (ANN), a variety of performance metrics were employed. Among these metrics were the mean square error (MSE), which calculates the average squared discrepancy between the predicted and observed values (Eq. (1)), and the regression coefficient (R), which measures the magnitude and direction of the linear association between the predicted and observed values (Eq. (2)) [46–49].Furthermore, an analysis of variance (ANOVA) was conducted to further evaluate the performance of the ANN.

In addition, an iterative approach was adopted to optimize the performance of the ANN. This iterative method sought to reduce the MSE and improve the correlation coefficients across the training, validation, and testing stages. Through continuous modification of the ANN parameters based on performance assessment, the objective was to enhance the network's capacity to accurately predict the desired results. Consequently, this iterative procedure enhanced the effectiveness and dependability of the ANN.

$$MSE = \frac{1}{n}\sum_{t=1}^{n}\left(y - y'\right)^2 \quad (1)$$

$$R = \frac{n\sum_{i=1}^{n}\left(y'y\right) - \left[\sum_{i=1}^{n} y'\right]\left[\sum_{i=1}^{n} y\right]}{\sqrt{\left[n\sum_{i=1}^{n} y^2 - \left[\sum_{i=1}^{n} y^2\right]\right]\left[n\sum_{i=1}^{n} y'^2 - \left[\sum_{i=1}^{n} y'^2\right]\right]}} \quad (2)$$

where *n* is the number of observations, *y* are the actual results (simulation outputs), and *y'* are the predicted targets (ANN outputs).

3. Results and discussion

3.1. Simulation validation

The validation phase of the simulation conducted in DWSIM entailed a comparison with the investigation performed by Guang et al. [17]. Tables 5 and 6 were utilized to outline the discrepancies in the mole fractions and temperatures of significance within their respective distillation columns. It is noteworthy that these discrepancies remained below 5%.

3.2. Sensitivity analysis

Sensitivity analyses, outlined in Appendix B, were conducted to identify the variables that had a substantial impact on the target compounds. Tables 7 and 8 show the inputs and outputs employed in the ANN design.

3.3. Design and training of the ANN

Following the sensitivity analysis, the design of the ANN was conducted (Fig. 3), incorporating six (6) input variables: feed temperature (T-in), IPA molar fraction (IPA-in), DIPE molar fraction (DIPE-in), pressure of Column-1(P CSCOL-1), pressure of Column-2 (P CSCOL-2), pressure of Column-3 (P CSCOL-3); and four (4) output variables: IPA mole fraction from the bottom of Column-2 (X_IPA-C2), DIPE mole fraction from the bottom of Column-3 (X_DIPE-DC3), IPA

Table 5. Simulation Validation (Mole fractions)

Column	Parameter	Guang et al. [17]	DWSIM	Error (%)
CSCOL-1	DIPE (distillate)	0.541	0.533	1.50
	Water (bottom)	0.999	0.988	1.2
CSCOL-2	DIPE (distillate)	0.658	0.645	2.02
	IPA (bottom)	0.999	0.993	0.6
CSCOL-3	DIPE (distillate)	0.620	0.605	2.42
	DIPE (bottom)	0.999	0.999	0

Table 6. Simulation Validation (Temperatures)

Column	Parameter	Guang et al. [17]	DWSIM	Error (%)
CSCOL-1	T (distillate)	308.20	308.02	0.058
	T (bottom)	368.52	385.20	4.520
CSCOL-2	T (distillate)	334.80	355.05	6.049
	T (bottom)	354.80	353.32	0.417
CSCOL-3	T (distillate)	387.50	387.00	0.127
	T (bottom)	328.00	342.13	4.307

Table 7. ANN inputs

Inputs			
Nomenclature	Parameter	Range	Unit
T-in	Feed temperature of all streams	200–315	K
IPA-in	Mole fraction of IPA feed stream	0.06–0.250	%
DIPE-in	Mole fraction of DIPE feed stream	0.06–0.250	%
P CSCOL-1	CSCOL-1 pressure	1.00–3.00	atm
P CSCOL-2	CSCOL-2 pressure	1.00–3.00	atm
P CSCOL-3	CSCOL-3 pressure	2.00–8.00	atm

Table 8. ANN ouputs

	Outputs			
	CSCOL-1	CSCOL-2	CSCOL-3	
	Distillate	Bottoms	Distillate	Bottoms
Mole fractions	IPA	IPA	DIPE	DIPE
Nomenclature	X_IPA-DC1	X_IPA-BC2	X_DIPE-DC3	X_DIPE-BC3
Unit	-	-	-	-

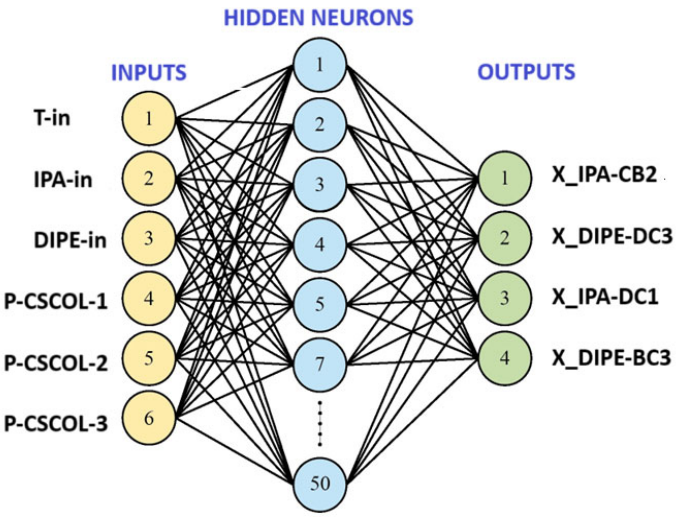

Fig. 3. Designed ANN.

mole fraction from the organic liquid of Column-1 (X_IPA-DC1), and DIPE mole fraction from the distillate of Column-3 (X_DIPE-BC3).

3.4. ANN topology

This section describes the design and structuring of the ANN by analyzing the correlation coefficient (R) and the MSE.

3.4.1. Selection of ANN training algorithm and the number of neurons in the hidden layer

The ANN architecture employed in this study used three training algorithms that have been previously demonstrated to be effective in minimizing the MSE loss function and maximize R: the Levenberg-Marquardt (LM), Bayesian regularization (BR), and scaled conjugate gradient back-propagation (SCG) algorithms [50–53].

After following a combined trial-and-error approach (Number of neurons was systematically altered to determine the impact of the architectural choice of the hidden layer) based on the best coefficient of determination R obtained during training, the selected trials along with their corresponding values of linear correlation (R) and mean squared error (MSE) for various ANN topologies are summarized in Table 9.

Based on the analysis, it is determined that the optimal structure of the ANN (with a minimum MSE of 7.60e-04 and maximum R of 0.99188) utilizes the Bayesian Regularization (BR) algorithm and features a hidden layer with 50 neurons. The advantage of a BR algorithm lies in its ability to predict complex relationships and make less biased decisions [50, 54, 55].

Table 9. Pearson's correlation coefficient (R) and mean square error (MSE) values

#	Levenberg-Marqua				Bayesian Regularization				Scale Conjugate Gradient			
Neu-rons	R Train	R Test	MSE train	MSE Test	R Rain	R Test	MSE Train	MSE Test	R Rain	R Test	MSE Train	MSE Test
10	9.74E-01	9.56E-01	4.83E-03	8.11E-03	9.71E-01	9.67E-01	5.33E-03	5.99E-03	9.56E-01	9.66E-01	8.15E-03	6.27E-03
20	9.64E-01	9.66E-01	6.46E-03	6.56E-03	9.88E-01	9.39E-01	2.28E-03	1.15E-02	9.62E-01	9.68E-01	6.89E-03	5.97E-03
30	9.81E-01	9.55E-01	3.42E-03	8.34E-03	9.90E-01	9.48E-01	1.80E-03	9.82E-03	9.68E-01	9.53E-01	5.90E-03	8.59E-03
40	9.71E-01	9.61E-01	5.26E-03	7.19E-03	9.94E-01	9.57E-01	1.15E-03	8.23E-03	9.68E-01	9.54E-01	5.90E-03	8.32E-03
50	9.73E-01	9.54E-01	5.05E-03	8.33E-03	9.97E-01	9.64E-01	7.60E-04	1.86E-03	9.72E-01	9.58E-01	4.82E-03	1.25E-02
60	9.76E-01	9.53E-01	4.42E-03	8.57E-03	9.38E-01	9.55E-01	4.14E-04	8.57E-03	9.73E-01	9.31E-01	4.85E-03	1.31E-02
70	9.08E-01	8.09E-01	1.51E-02	3.25E-02	9.50E-01	8.42E-01	3.31E-03	4.97E-02	8.92E-01	8.47E-01	1.73E-02	2.54E-02
80	9.47E-01	7.29E-01	8.79E-03	4.88E-02	9.87E-01	8.26E-01	2.18E-03	5.40E-02	8.89E-01	8.42E-01	1.83E-02	2.44E-02
90	9.91E-01	9.30E-01	1.75E-03	1.38E-02	9.93E-01	8.08E-01	1.24E-03	9.94E-02	9.72E-01	9.58E-02	1.10E-02	2.44E-02
100	9.31E-01	8.40E-01	1.10E-02	2.73E-02	9.09E-01	8.65E-01	5.36E-05	1.11E-01	9.30E-01	7.96E-02	1.12E-02	3.68E-02

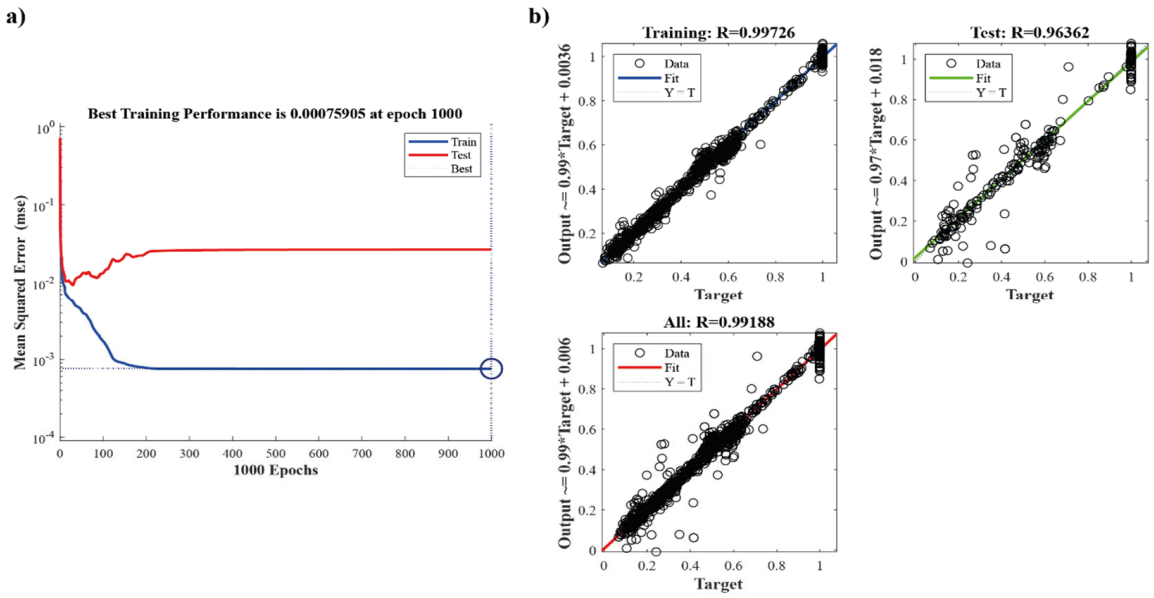

Fig. 4. MSE and R for the ANN.

3.4.2.ANN training and testing

The main validation tests for process modeling are the mean squared error (MSE) and the linear correlation coefficient R. Table 10 displays the parameter values for the training and testing phases of the ANN.

Table 10. R and MSE of ANN designed

Phase	MSE	R
Training	0.00076	0.997
Testing	0.00186	0.964

The training phase of the ANN yielded a remarkably low MSE score of 0.00076, while the testing phase resulted in a slightly higher MSE of 0.00186 (Table 10), both indicating the model's capability to generate precise predictions. Illustrated in Fig. 4a, the MSE progression demonstrates a consistent decrease in the training data towards zero, affirming the robust predictive performance of the ANN. Figure 4b displays R values for both training and testing phases, with values of 0.997 and 0.963 respectively, culminating in an overall R-value of 0.991. These notably high R-values denote a strong correlation between predicted outputs and actual targets. R-values nearing 1 signify the superior performance of the ANN. The validation process established benchmarks of R-values between 0.96 to 1 and MSE below 0.0020. By satisfying these criteria, the developed ANN emerges as a dependable and precise predictive model for the specified application.

3.5. Model prediction of X_{IPA}, X_{DIPE} in the columns: CSCOL-1, CSCOL-2 and CSCOL-3

Following the acquisition of predictions generated by the Artificial Neural Network (ANN), an interpretative process ensued, employing graphical analysis to juxtapose the experimental results derived from DWSIM (Experimental/Real) against the anticipated outcomes projected by the ANN (Predicted). This comparison was executed utilizing the identical set of 400 data points employed during the network's training phase.

3.5.1. IPA mole fraction from CSCOL-1 distillate

In the assessment of the X_{IPA} in the organic liquid phase of CSCOL-1 sample, the prediction obtained during training exhibits an average error of 7.28%. This discrepancy is primarily attributed to the low concentrations inherent in experimental data. Nonetheless, despite these errors, the predicted values demonstrate a substantial overlap with the experimental values, as illustrated in Fig. 5.

3.5.2. IPA mole fraction from CSCOL-2 bottom

The prediction of X_{IPA} from CSCOL-2 bottom yielded an average error of 6.22%, primarily attributed to the presence of outliers within the dataset. Figure 6 illustrates the alignment of predicted data points generated by the neural network with the corresponding experimental data points, demonstrating the model's fitting performance.

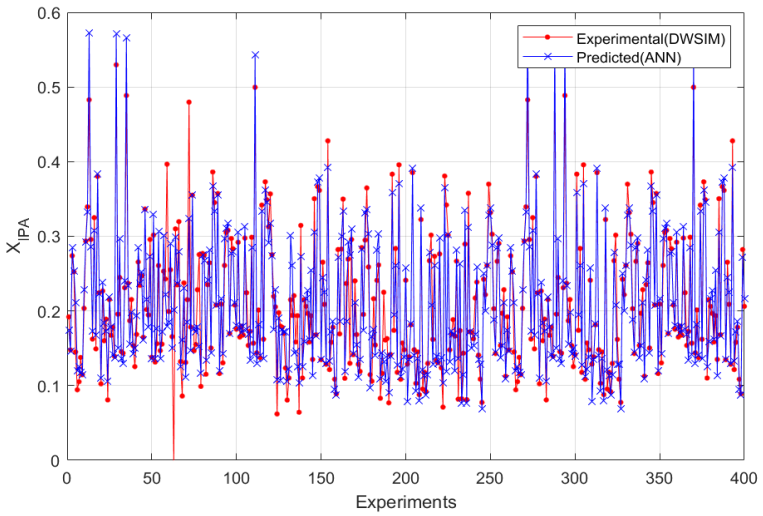

Fig. 5. X_{IPA} prediction in CSCOL-1 (distillate).

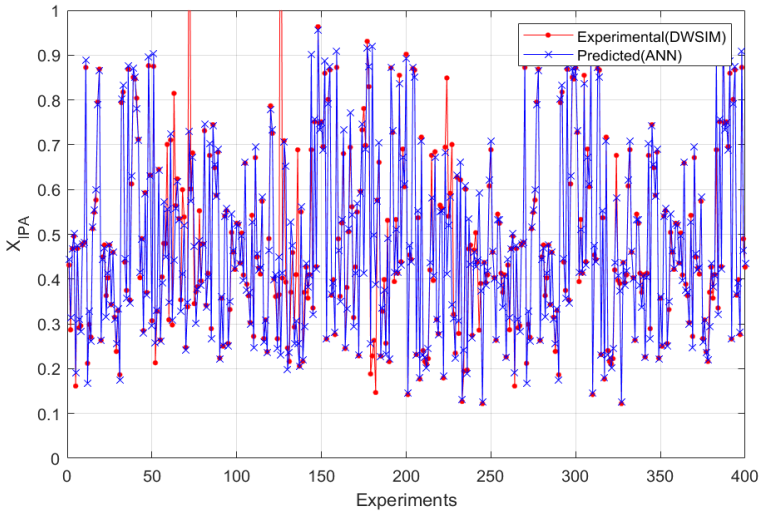

Fig. 6. X_{IPA} prediction in CSCOL-2 (bottom).

3.5.3. DIPE mole fraction from CSCOL-3 bottom

Figure 7 displays the predicted X_{DIPE} during the training phase of the ANN, exhibiting significant overlap with most of the database concerning the experimental data. The average prediction error stands at 2.54%, indicative of the robust fitting performance achieved during the network's training phase.

3.5.4. DIPE mole fraction from CSCOL-3 distillate

In the distillate of CSCOL-3, the prediction error for X_{DIPE} stands at 4.80%. As depicted in Fig. 8, there is a notable alignment between the predicted and experimental data points, affirming the ANN's accurate prediction capabilities.

3.6. ANN model verification

The predictive performance of the artificial neural network (ANN) for X_{IPA} and X_{DIPE} within the CSCOL-1, CSCOL-2, and CSCOL-3 columns was assessed using a dataset comprising 25 randomly selected input variables, including feed temperature (T-in), IPA molar fraction (IPA-in), DIPE molar fraction (DIPE-in), and pressures of CSCOL-1, CSCOL-2, and CSCOL-3 (P CSCOL-1, P CSCOL-2, P CSCOL-3). These inputs were not previously encountered by the ANN during training. The average prediction error was less than 10%, which reveals a close correspondence between the experimental observations and the ANN predictions, indicative of the network's robust predictive capabilities concerning both distillate and residue mole fractions from the distillation columns, as depicted in Fig. 9.

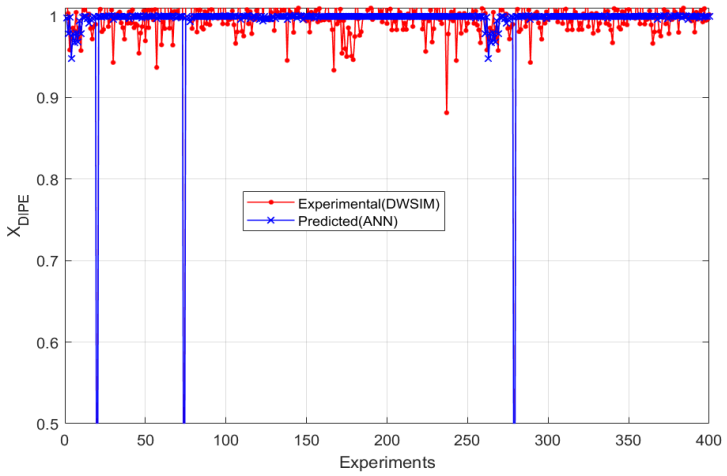

Fig. 7. X_{DIPE} prediction in CSCOL-3 (bottom).

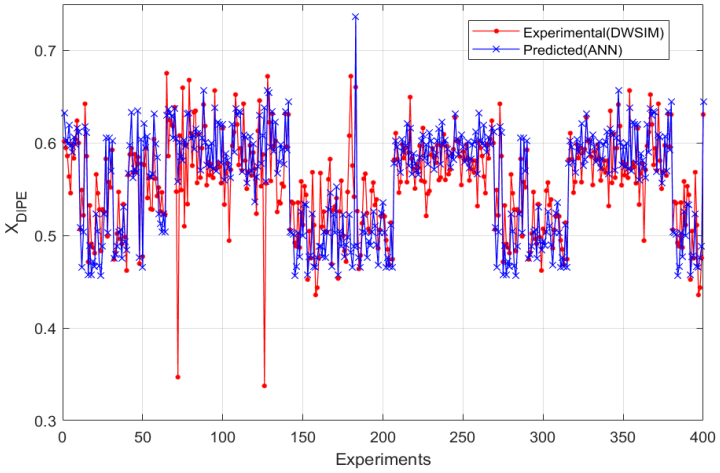

Fig. 8. X_{DIPE} prediction in CSCOL-3 (distillate).

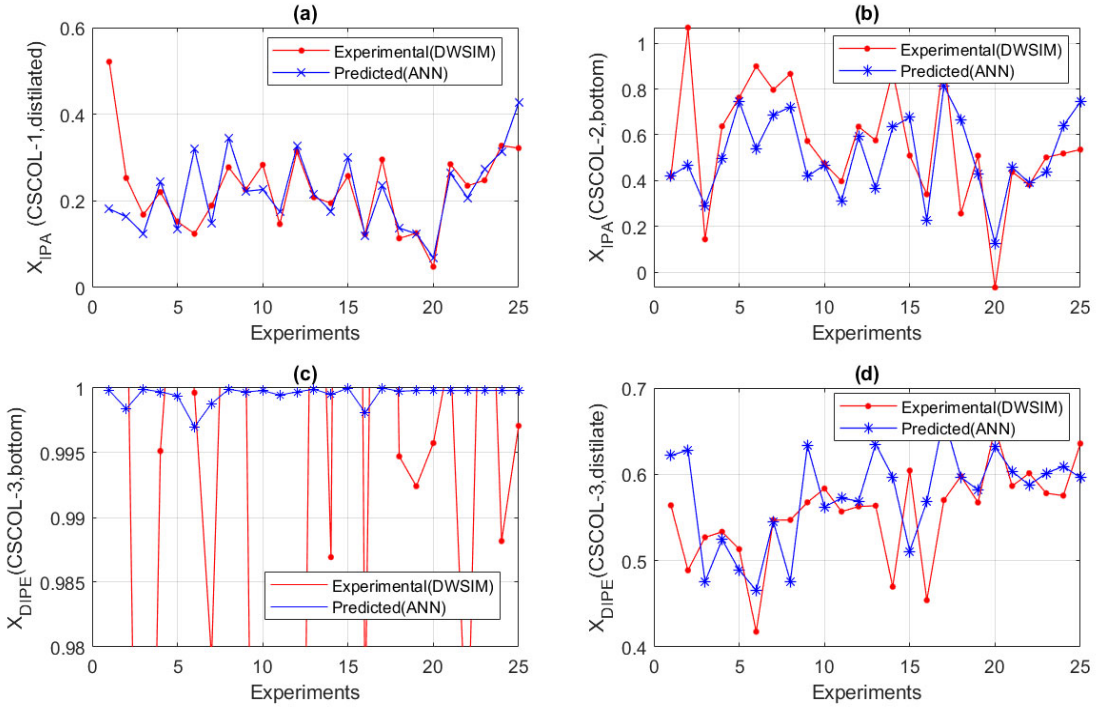

Fig. 9. Comparison between experimental and prediction data-EDC: a) X_{IPA} prediction in CSCOL-1 (distillate), b) X_{IPA} prediction in CSCOL-2 (bottom), c) X_{DIPE} prediction in CSCOL-3 (bottom), d) X_{DIPE} prediction in CSCOL-3 (distillate).

Table 11. ANOVA

Source	Sum of squares	DOF	Mean square	F-Value	P-value
		X_{IPA} prediction in CSCOL-1 (distillate)			
Inter groups	0.00408015	1	0.00408015	0.42	0.5207
Intra groups	0.467761	4	0.00974502		
Total (Corr.)	0.471841	49			
		X_{IPA} prediction in CSCOL-2 (bottom)			
Inter groups	0.0446808	1	0.0446808	1.16	0.2865
Intra groups	1.84638	48	0.0384663		
Total (Corr.)	1.89106	49			
		X_{DIPE} prediction in CSCOL-3 (bottom)			
Inter groups	0.000133588	1	0.000133588	0.24	0.6236
Intra groups	0.0262873	48	0.000547651		
Total (Corr.)	0.0264209	49			
		X_{DIPE} prediction in CSCOL-3 (distillated)			
Inter groups	0.00685952	1	0.00685952	2.24	0.1414
Intra groups	0.14728	48	0.00306834		
Total (Corr.)	0.15414	49			

In this study, we employed ANOVA functions to conduct statistical validation of the ANN. The outcomes of the ANOVA analysis are presented in Table 11, where all P-values (representing the probability value in statistical significance tests) exceed 0.05. This suggests an absence of statistically significant disparities between the means of the observed data and the predictions generated by the ANN. Therefore, based on this statistical test, it can be inferred that the constructed ANN is statistically reliable for the prediction of X_{IPA}, X_{DIPE} in the columns: CSCOL-1, CSCOL-2 and CSCOL-3, with a confidence level of 95%.

The model correctly reproduced the technical behavior of the Isopropanol/Water azeotropic system under different operating conditions. As detailed in Appendix B, variations in operating parameters strongly affected separation performance: increasing the feed temperature from 200 to 315 K reduced the IPA fraction in the distillate by about 19%, raising the IPA content in the feed enhanced its recovery up to 240%, higher DIPE concentrations decreased the IPA fraction by 28%, and in CSCOL-1, increasing the pressure from 1.0 to 3.0 atm reduced the distillate IPA fraction by 50%, consistent with the thermodynamic promotion of azeotrope stability at higher pressures. These behaviors were consistently reproduced by the ANN, confirming its ability to capture the observed separation behavior and to serve as a reliable tool for process analysis. However, determining truly optimal operating parameters requires a detailed optimization framework, which is beyond the scope of the present study and will be addressed in future research, with an emphasis on energy efficiency and environmental performance.

3.7. Recommended steps for ANN implementation

Figure 10 illustrates a comprehensive schematic outlining the sequential procedures and requisite measures essential for integrating an artificial neural network (ANN) into an industrial workflow. The subsequent recommendations are proposed for the seamless integration of ANN into real-time applications: delineate the objectives of the ANN (whether for Quality Control or Process Optimization); establish a historical database suitable for retraining the ANN; preprocess the database to ensure compatibility with ANN training requirements; conduct rigorous training of the ANN using appropriate algorithms; integrate the ANN into hardware components seamlessly integrated into the automated process control system; institute mechanisms for real-time monitoring of ANN performance; periodically update the ANN utilizing feedback loops to facilitate continuous enhancement; implement security protocols based on the prognostic capabilities of the ANN; and thoroughly document the entire integration process for comprehensive understanding and future reference.

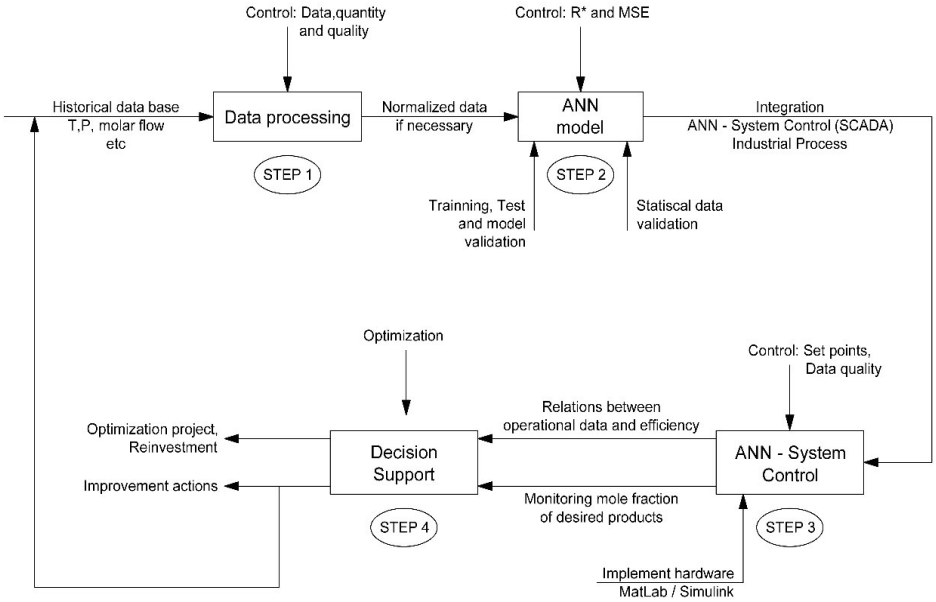

Fig. 10. Generalized diagram to implement the ANN. Source [53, 56, 57].

4. Conclusions

In this research, an artificial neural network (ANN) was developed to predict the molar fractions of isopropanol (IPA) and diisopropyl ether (DIPE) in a pressure-swing azeotropic distillation system. The database used to train the ANN was generated from the validation of a simulation. The ANN architecture consists of 50 hidden neurons and 6 input variables: feed temperature, IPA molar fraction in the feed, DIPE molar fraction in the feed, and the pressures of the three columns. The ANN is capable of predicting four output variables: IPA molar fraction in the bottom of Column 2, DIPE molar fraction in the bottom of Column 3, IPA molar fraction in the organic liquid of Column 1, and DIPE molar fraction in the distillate of Column 3.

The training of the ANN was carried out using the Bayesian regularization algorithm, obtaining a test mean squared error of 0.00186 and a correlation coefficient of 0.964. An analysis of variance (ANOVA) was performed to compare the experimental data (DWSIM) with the values predicted by the ANN, validating its accuracy in predicting the molar fractions with a significance level of 95%. The results suggest that the developed ANN has potential as a predictive tool to optimize the separation efficiency of IPA/water mixtures through pressure-swing distillation, a process used in the manufacturing of products such as paints, varnishes, inks, adhesives, and cleaners.

To implement the ANN in real-time, it is recommended to clearly define the objectives, establish a historical database for retraining, preprocess the data, train the ANN, integrate it into the automatic process control system, monitor its performance, continuously update it through feedback cycles, implement safety measures based on ANN predictions, and exhaustively document the process. In future research, computationally efficient and low-cost strategies will be sought for the real-time implementation of artificial neural networks, as well as the application of genetic optimization algorithms to ANNs using hybrid approaches, considering energy efficiency and environmental impact parameters. Compared with conventional simulations, ANNs provide higher predictive accuracy, lower computational cost, and the ability to capture nonlinearities without explicit thermodynamic or kinetic models. Their main limitations are the need for large, representative, high-quality datasets and reduced interpretability relative to first-principles models. Accordingly, ANNs are best used as complementary tools to conventional modeling, especially when rapid, reliable predictions and optimization support are required.

References

[1]. G. Moreno-Cedeño, N. Tellería-Mata, S. Villanueva, M. Henríquez, Tech note: technologies for the production of isopropyl alcohol (IPA) / Nota técnica: tecnologías para la producción de alcohol isopropílico (IPA), (2019).

[2]. W.J. Chua, G.P. Rangaiah, K. Hidajat, Design and optimization of isopropanol process based on two alternatives for reactive distillation, *Chem. Eng. Process.: Process Intensif.* 118 (2017) 108–116. DOI: 10.1016/j.cep.2017.04.021

[3]. C. Guang, X. Shi, Z. Zhang, et al., Comparison of heterogeneous azeotropic and pressure-swing distillations for separating the diisopropylether/isopropanol/water mixtures, *Chem. Eng. Res. Des.* 143 (2019) 249–260. DOI: 10.1016/J.CHERD.2019.01.021

[4]. H. Hasanudin, W.R. Asri, L. Andini, et al., Enhanced Isopropyl Alcohol Conversion over Acidic Nickel Phosphate-Supported Zeolite Catalysts, *ACS Omega* 7 (2022) 38923–38932. DOI: 10.1021/ACSOMEGA.2C04647

[5]. A. Yang, S. Jin, W. Shen, et al., Investigation of energy-saving azeotropic dividing wall column to achieve cleaner production via heat exchanger network and heat pump technique, *J. Clean. Prod.* 234 (2019) 410–422. DOI: 10.1016/j.jclepro.2019.06.224

[6]. E. Palacio González, L.M. Tamayo, M. Asesor, J. Sebastián Gómez, (2013). Separación ternaria de una mezcla azeotrópica isopropanol - agua.

[7]. H. Xia, Q. Ye, S. Feng, et al., A novel energy-saving pressure swing distillation process based on self-heat recuperation technology, *Energy* 141 (2017) 770–781. DOI: 10.1016/j.energy.2017.09.108

[8]. V.N. Kiva, E.K. Hilmen, S. Skogestad, Azeotropic phase equilibrium diagrams: a survey, *Chem. Eng. Sci.* 58 (2003) 1903–1953. DOI: 10.1016/S0009-2509(03)00018-6

[9]. I.Q. Matos, J.S. Varandas, J.P.L. Santos, Thermodynamic modeling of azeotropic mixtures with [EMIM][TFO] with cubic-plus-association and cubic EOSS, *Braz. Soc. Chem. Eng.* 35 (2018) 363–372. DOI: 10.1590/0104-6632.20180352s20160025

[10]. A. Avilés-Martínez, N. Medina-Herrera, A. Jiménez-Gutiérrez, et al., Risk Analysis Applied to Bioethanol Dehydration Processes: Azeotropic Distillation versus Extractive Distillation, *Comput. Aided Chem. Eng.* 37 (2015) 1835–1840. DOI: 10.1016/B978-0-444-63577-8.50151-0

[11]. J. Acosta, A. Arce, J. Martínez-Ageitos, et al., Vapor−Liquid Equilibrium of the Ternary System Ethyl Acetate + Hexane + Acetone at 101.32 kPa, J. *Chem. Eng. Data* 47 (2002) 849–854. DOI: 10.1021/je0102917

[12]. A. Iqbal, S.A. Ahmad, Pressure swing distillation of azeotropic mixture – A simulation study, *Perspect. Sci.* 820 (2016) 4–6. DOI: 10.1016/j.pisc.2016.01.001

[13]. J. Buitrago, D. Amaya, O. Ramos, Model and simulation of a hydrotreatment reactor for diesel hydrodesulfurization in oil refining, *Contemp. Eng. Sci.* 10 (2017) 1245–1254. DOI: 10.12988/ces.2017.710135

[14]. M.W. Niu, G.P. Rangaiah, Process Retrofitting via Intensification: A Heuristic Methodology and Its Application to Isopropyl Alcohol Process, *Ind. Eng. Chem. Res.* 55 (2016) 3614–3629. DOI: 10.1021/acs.iecr.5b02707

[15]. Y. Xu, K.T. Chuang, A.R. Sanger, Design of a Process for Production of Isopropyl Alcohol by Hydration of Propylene in a Catalytic Distillation Column, *Chem. Eng. Res. Des*. 80 (2002) 686–694. DOI: 10.1205/026387602760312908

[16]. S. Arifin, I.L. Chien, Combined preconcentrator/recovery column design for isopropyl alcohol dehydration process, *Ind. Eng. Chem. Res.* 46 (2007) 2535–2543. DOI: 10.1021/ie061446c

[17]. C. Guang, X. Zhao, Z. Zhang, et al., Optimal design and performance enhancement of heteroazeotropic and pressure-swing coupling distillation for downstream isopropanol separation, *Sep. Purif. Technol.* 242 (2020) 116836. DOI: 10.1016/j.seppur.2020.116836

[18]. F. Shi, J. Gao, X. Huang, An affine invariant approach for dense wide baseline image matching, *Int. J. Distrib. Sens. Netw.*, 2016. DOI: 10.1177/1550147716680826

[19]. Q. Guo, Z. He, Z. Wang, Simulating daily $PM_{2.5}$ concentrations using wavelet analysis and artificial neural network with remote sensing and surface observation data, *Chemosphere* 340 (2023) 139886. DOI: 10.1016/j.chemosphere.2023.139886

[20]. A.A. Elgibaly, M. Ghareeb, S. Kamel, M. El-Sayed El-Bassiouny, Prediction of gas-lift performance using neural network analysis, *AIMS Energy* 9 (2021) 355–378. DOI: 10.3934/energy.2021019

[21]. Q. Guo, Z. He, Z. Wang, Predicting of Daily PM2.5 Concentration Employing Wavelet Artificial Neural Networks Based on Meteorological Elements in Shanghai, China, *Toxics* 11 (2023) 51. DOI: 10.3390/toxics11010051

[22]. M. Hamdi, H.A. El Salmawy, R. Ragab, Optimum configuration of a dispatchable hybrid renewable energy plant using artificial neural networks: Case study of Ras Ghareb, Egypt, *AIMS Energy* 11 (2023) 171–196. DOI: 10.3934/energy.2023010

[23]. Q. Guo, Z. He, Z. Wang, Prediction of monthly average and extreme atmospheric temperatures in Zhengzhou based on artificial neural network and deep learning models, *Front. For. Glob. Change* 6 (2023). DOI: 10.3389/ffgc.2023.1249300

[24]. A.A. Aly, B. Saleh, M.M. Bassuoni, et al., Artificial neural network model for performance evaluation of an integrated desiccant air conditioning system activated by solar energy, *AIMS Energy* 7 (2019) 395–412. DOI: 10.3934/ENERGY.2019.3.395

[25]. Q. Guo, Z. He, Prediction of the confirmed cases and deaths of global COVID-19 using artificial intelligence. *Environ. Sci. Pollut. Res.* 28 (2021) 11672–11682. DOI: 10.1007/s11356-020-11930-6

[26]. Z. He, Q. Guo, Z. Wang, X. Li, Prediction of Monthly PM2.5 Concentration in Liaocheng in China Employing Artificial Neural Network, A*tmosphere* 13 (2022). DOI: 10.3390/atmos13081221

[27]. Q. Guo, Z. He, Z. Wang, Prediction of Hourly PM2.5 and PM10 Concentrations in Chongqing City in China Based on Artificial Neural Network, *Aerosol Air Qual. Res.* 23 (2023). DOI: 10.4209/aaqr.220448

[28]. A. Kandil, S. Khaled, T. Elfakharany, Prediction of the equivalent circulation density using machine learning algorithms based on real-time data, *AIMS Energy* 11 (2023) 425–453. DOI: 10.3934/energy.2023023

[29]. Q. Guo, Z. He, S. Li, et al., Air Pollution Forecasting Using Artificial and Wavelet Neural Networks with Meteorological Conditions, *Aerosol Air Qual. Res.* 20 (2020) 1429–1439. DOI: 10.4209/aaqr.2020.03.0097

[30]. M. Pirdashti, S. Curteanu, M.H. Kamangar, et al., Artificial neural networks: applications in chemical engineering, *Rev. Chem. Eng.* 29 (2013) 205–239. DOI: 10.1515/revce-2013-0013

[31]. J. Panerati, M.A. Schnellmann, C. Patience, et al., Experimental methods in chemical engineering: Artificial neural networks–ANNs, *Can. J. Chem. Eng.* 97 (9) (2019) 2372–2382. DOI: 10.1002/cjce.23507

[32]. V.M. Cristea, M. Baigulbayeva, Y. Ongarbayev, et al., Prediction of Oil Sorption Capacity on Carbonized Mixtures of Shungite Using Artificial Neural Networks, *Processes* 11 (2023) 518. DOI: 10.3390/PR11020518

[33]. D.M. Himmelblau, Applications of artificial neural networks in chemical engineering, *Korean J. Chem. Eng.* 17 (2000) 373–392. DOI: 10.1007/BF02706848

[34]. Y. Shin, R. Smith, S. Hwang, Development of model predictive control system using an artificial neural network: A case study with a distillation column, *J. Clean. Prod.* 277 (2020) 124124. DOI: 10.1016/j.jclepro.2020.124124

[35]. L.M. Ochoa-Estopier, M. Jobson, R. Smith, Operational optimization of crude oil distillation systems using artificial neural networks, *Comput. Chem. Eng.* 59 (2013) 178–185. DOI: 10.1016/j.compchemeng.2013.05.030

[36]. A.C. Dimian, C.S. Bildea, A.A. Kiss, Introduction in Process Simulation, *Comput. Aided Chem. Eng*. 35 (2014) 35–71. DOI: 10.1016/B978-0-444-62700-1.00002-4

[37]. A.A. Kiss, Advanced distillation technologies - Design, Control and Applications, First, Wiley, Noida, India., 2013. DOI: 10.1002/9781118543702

[38]. G. Soave, S. Gamba, L.A. Pellegrini, SRK equation of state: Predicting binary interaction parameters of hydrocarbons and related compounds, *Fluid Ph. Equilibria* 299 (2010) 285–293. DOI: 10.1016/j.fluid.2010.09.012

[39]. Z. Feng, W. Shen, G.P. Rangaiah, L. Dong, Design and control of vapor recompression assisted extractive distillation for separating n-hexane and ethyl acetate, *Sep. Purif. Technol*. 240 (2020) 116655. DOI: 10.1016/j.seppur.2020.116655

[40]. Z. Chen, Z. Zhang, J. Zhou, et al., Efficient Synthesis of Isobutylene Dimerization by Catalytic Distillation with Advanced Heat-Integrated Technology, *Ind. Eng. Chem. Res*. 60 (2021) 6121–6136. DOI: 10.1021/acs.iecr.1c00945

[41]. V. Singh, I. Gupta, H.O. Gupta, ANN based estimator for distillation—inferential control, *Chem. Eng. Process.: Process Intensif.* 44 (2005) 785–795. DOI: 10.1016/j.cep.2004.08.010

[42]. F. Pedregosa, G. Varoquaux, A. Gramfort, et al., Scikit-learn: Machine Learning in Python. Journal of Machine Learning Research, 12 (2011) 2825–2830. https://www.jmlr.org/papers/v12/pedregosa11a.html

[43]. M.D. Bloice, A. Holzinger, A Tutorial on Machine Learning and Data Science Tools with Python. In: Holzinger, A. (eds) Machine Learning for Health Informatics. Lecture Notes in Computer Science (2016), vol 9605. Springer, Cham. DOI: 10.1007/978-3-319-50478-0_22

[44]. A. Hafiz Al Hariri, A.E. Khalifa, M. Talha, et al., Artificial neural network and differential evolution optimization of a circulated permeate gap membrane distillation unit, *Sep. Purif. Technol*. 338 (2024) 126517. DOI: 10.1016/J.SEPPUR.2024.126517

[45]. Y. Chen, L. Song, Y. Liu, et al., A Review of the Artificial Neural Network Models for Water Quality Prediction, *Appl. Sci.* 10 (2020) 5776. DOI: 10.3390/APP10175776

[46]. L. Zhang, X. Sun, S. Gao, Temperature prediction and analysis based on improved GA-BP neural network, *AIMS Environ. Sci.* 9 2022 735–753. DOI: 10.3934/ENVIRONSCI.2022042

[47]. L. Wang, B. Wu, Q. Zhu, Y.R. Zeng, Forecasting Monthly Tourism Demand Using Enhanced Back propagation Neural Network, *Neural Process. Lett.* 52 (2020) 2607–2636. DOI: 10.1007/s11063-020-10363-z

[48]. K. Suphawan, K. Chaisee, Gaussian process regression for predicting water quality index: A case study on Ping River basin, Thailand, *AIMS Environ. Sci.* 8 (2021) 268–282. DOI: 10.3934/environsci.2021018

[49]. O. Narivs'kyi, R. Atchibayev, A. Kemelzhanova, et al., Mathematical Modeling of the Corrosion Behavior of Austenitic Steels in Chloride-Containing Media During the Operation of Plate-Like Heat Exchangers, *Eurasian Chem.-Technol. J.* 24 (2022) 295–301. DOI: 10.18321/ectj1473

[50]. M. Kayri, Predictive Abilities of Bayesian Regularization and Levenberg-Marquardt Algorithms in Artificial Neural Networks: A Comparative Empirical Study on Social Data, *Math. Comput. Appl.* 21 (2016) 20. DOI: 10.3390/mca21020020

[51]. S. Bharati, M. Rahman, P. Podder, et al., Comparative Performance Analysis of Neural Network Base Training Algorithm and Neuro-Fuzzy System with SOM for the Purpose of Prediction of the Features of Superconductors. In: Abraham, A., Siarry, P., Ma, K., Kaklauskas, A. (eds) Intelligent Systems Design and Applications. ISDA 2019. Advances in Intelligent Systems and Computing, 1181 (2021). Springer, Cham. DOI: 10.1007/978-3-030-49342-4_7

[52]. L.M. Saini, Peak load forecasting using Bayesian regularization, Resilient and adaptive backpropagation learning based artificial neural networks, *Electr. Power Syst. Res.* 78 (2008) 1302–1310. DOI: 10.1016/j.epsr.2007.11.003

[53]. D. Chuquin-Vasco, G. Torres-Yanacallo, C. Calderón-Tapia, et al., ANN for the prediction of isobutylene dimerization through catalytic distillation for a preliminary energy and environmental evaluation, *AIMS Environ. Sci.* 11 (2024) 157–183. DOI: 10.3934/environsci.2024009

[54]. A. Suliman, B. Omarov, Applying Bayesian Regularization for Acceleration of Levenberg-Marquardt based Neural Network Training, *Int. J. Interact. Multimed. Artif. Intell.* 5 (2018) 68. DOI: 10.9781/ijimai.2018.04.004

[55]. H. Garoosiha, J. Ahmadi, H. Bayat, The assessment of Levenberg–Marquardt and Bayesian Framework training algorithm for prediction of concrete shrinkage by the artificial neural network, *Cogent Eng.* 6 (2019) 1609179. DOI: 10.1080/23311916.2019.1609179

[56]. D. Chuquín-Vasco, J. Osorio-Getial, N. Chuquín-Vasco, et al., Computational Modeling and Machine Learning for Predicting the Volumetric Flows in Crude Distillation Units: A Detailed Simulation and Validation Approach, *Eurasian Chem.-Technol. J.* 27 (2025) 111–125. DOI: 10.18321/ectj1659

[57]. D. Chuquin-Vasco, D. Chicaiza-Sagal, C. Calderón-Tapia, et al., Forecasting mixture composition in the extractive distillation of n-hexane and ethyl acetate with n-methyl-2-pyrrolidone through ANN for a preliminary energy assessment, *AIMS Energy* 12 (2024) 439–463. DOI: 10.3934/energy.2024020